Experimental evidence of enhanced adsorption dynamics at liquid-liquid interfaces under electric field

Sameer Mhatre,[*,†,‡] Sébastien Simon,[†] and Johan Sjöblom[†]

†*Ugelstad Laboratory, Department of Chemical Engineering, Norwegian University of Science and Technology (NTNU), NO-7491 Trondheim, Norway*

‡*Department of Chemical and Petroleum Engineering, Schulich School of Engineering, University of Calgary, Calgary, Canada T2N 1N4*

E-mail: sameer.mhatre@ucalgary.ca

Abstract

In this work we investigate adsorption of surface active compounds at water-oil interface subjected to an electric field. A fluid system comprising a pendent water drop surrounded by an asphaltene-rich organic phase is exposed to a DC uniform electric field. Two sub-fractions of asphaltenes having contrasting affinities to water-oil interface are used as surface active compounds. The microscopic changes in the drop shape, as a result of asphaltene adsorption, are captured and the drop profiles are analyzed by using our in-house code for axisymmetric drop shape analysis (ADSA) under electric field. The estimates of dynamic interfacial tension under different strengths of the field (E_0) and concentrations of the asphaltene sub-fractions (C) are used to calculate adsorption dynamics and surface excess. The experimental observations and careful analysis of the data suggest that the externally applied electric field significantly stimulates the mass transfer rate at a liquid-liquid interface. The enhancement in mass transport at

water-oil interface can be attributed to the axisymmetric electrohydrodynamic fluid flows generated on either sides of the interface. The boost in mass transport is evident from the growing decay in equilibrium interfacial tension (γ_{eq}) and increased surface excess (Γ_{eq}) upon increasing strength of the applied electric field. The mass transfer intensification does not increase monotonously with the electric field strength above an optimum E_0, which is in agreement with previous theoretical studies in the literature. However, these first explicit experimental measurements of adsorption at an interface under electric field suggest that the optimum E_0 is determined by characteristics of the surface active molecules.

Introduction

The surfactants and their effects on fluid interfaces and multi-phase systems are well known and extensively investigated. In a multi-phase system the surface active compounds diffuse through fluids and adsorb at the empty sites of the interface forming a monolayer. The resulting changes in the interfacial properties depend on molecule's self-diffusivity and adsorption/desorption energy barriers at the interface.[1] Intermolecular interaction at the interface can be significant.[2] The mass transfer to the interface is a function of bulk concentration and can turn from diffusion controlled to kinetic-diffusion controlled as the concentration rises. As the surface coverage builds up the kinetics of adsorption and desorption are substantially governed by the interfacial concentration than the bulk concentration.[3] The probability of molecular adsorption to the interface is broadly defined by two models.[3,4] The diffusion controlled model states diffusion of molecules from the bulk phase to an imaginary subsurface near the interface followed by adsorption without much resistance. Here the diffusion from bulk to the subsurface is rate controlling the dynamic interfacial tension. However, the mixed kinetic-diffusion model is based on resistance to adsorption after molecules enter in to the subsurface. The diffusion from bulk is fast but the resistance to adsorb to the interface is strong on account of different factors. It also makes the un-adsorbed molecules to leave the

subsurface and diffuse back in to the bulk. There are a variety of theories that can estimate the interfacial concentration of surface active compounds (called surface excess) based on experimentally measured dynamic surface/interfacial tension.[1,3]

The mass and heat transfer at fluid interfaces are believed to boost when the interface is put into an electric field. When the electric field is imposed to a dielectric drop surrounded by another dielectric fluid, symmetric fluid circulations are induced inside the drop phase.[5] The electrical conductivities and permittivities of the drop and medium phases govern the direction of the circulations i.e. either from the drop's poles to equator or from equator to poles. The scientific investigations in the effect of applied electric field on mass/heat transport at fluid interfaces have been limited to theoretical studies. Assuming the resistance to the transport on the either side of interface, increasing Peclet number ($=\frac{advective\ transport\ rate}{diffusive\ transport\ rate}$) observed to increase the Nusselt number ($=\frac{convective\ heat\ transfer}{conductive\ heat\ transfer}$) and mass transfer Nusselt number (or Sherwood number) ($=\frac{convective\ mass\ transfer\ rate}{diffusion\ rate}$). Majority of the studies concluded that there exist a maximum steady state Nusselt number above which the heat/mass transport becomes independent of the Peclet number. The theoretical analyses by Morrison[6] and Griffiths *et al.*[7] considered the resistance to the transport lies outside the drop (called 'the external problem') and concluded that the mass and heat transfer are constant whether the flow circulations are from drop's poles to equator or in the reverse direction. The numerical studies by Oliver *et al.*[8,9] dealt with heat transfer when the transport resistance exists inside the drop phase ('the internal problem'). The effect of externally applied electric field is stronger when the drop is translating in comparison with a stationary drop. Relatively recent theoretical studies by Abdelaal and Jog[10–12] drew similar conclusions. The enhancement in heat and mass transfer ceases if the electric field is increased above an optimum field strength.[12] In the internal as well as the external problems for stationary and translating drops, depending on the Peclet number, different attributes of the applied electric field such as uniformity, non-uniformity, DC, AC, etc. are found to be affecting the transfer rates distinctly.

Previous studies in the literature reported observations that suggested stimulation of mass transfer at liquid interfaces under electric field.[13–16] However, these studies either lacked thorough analysis of the observations or were inconclusive. Some earlier studies speculated that a rise in ion density at a fluid interface under electric field is responsible for altered surface tension.[17–19] A liquid drop surrounded by another immiscible liquid and exposed to an electric field assumes a new shape. Moriya *et al.*[20] reported time dependent stretching of polyethylene oxide pendent drops under AC electric fields. Similar changes in electrified water drops and polysiloxane capsules, in the presence of additives that impart charge to the drop interfaces, were observed by Degan *et al.*[21] Their rheological measurements are debatable as it is not clear if they considered electric stresses in their experimental measurements. Weatherley *et al.*[22] observed flow currents at a flat liquid-liquid interface when an electric field was applied across it. We recently showed that a pendent water drop held in an asphaltene solution stretches in the vertical direction as the molecular density at its interface grows with time.[23] When the populating drop interface is exposed to a constant DC electric field- applied in the direction perpendicular to the drop's vertical axis- the stretching in the vertical direction was observed to be magnified with the field strength. When an electric field is applied to a water drop in an organic medium, the drop shows an instantaneous deformation in the direction of the applied field. However, the time-dependent vertical stretching of a pendent water drop in an asphaltene-rich phase indicated the evolving interfacial properties due to the applied field.

A freshly drilled crude oil contains a significant amount of water which is emulsified in the form of tiny droplets. In addition to it, fresh water is added in refinery operations to get rid of water-soluble compounds which is called desalting operation. The crude oil emulsions are kinetically stable given very small size of the dispersed water droplets and water-oil interface populated with indigenous surface active species. The polar molecules including asphaltenes, resins, naphthenic acids as well as fine solids[24] adsorb to the water-oil interface altering its properties and making the emulsion extremely difficult to separate

by gravitational settling. The asphaltene molecules are believed to irreversibly occupy the water-oil interface.[25] The resulting rigid skin is responsible for stable interface and inhibits drop-drop contact and merging. Understanding mechanism of the interfacial stabilization and its mitigation is paramount in refinery operations where the water content must be reduced to a specific level in order to make it suitable for fractionation.[26]

The experimental investigation of mass transfer at a liquid-liquid interface under electric field involves several technical difficulties.[15] The drop profile analysis could be an easier and straightforward method provided the interfacial properties of an interface under electric field are directly measured. This paper demonstrates experimental observations on enhanced mass transport at a water-oil interface when exposed to an electric field. Here we used two sub-fractions of asphaltenes as surface active molecules and axisymmetric drop shape analysis (ADSA) to measure the dynamic interfacial tension. ADSA is an excellent method to monitor time dependent interfacial properties. It has been extensively used to investigate mass transport at liquid interfaces by taking images of a sessile or pendent drop to capture any microscopic change in its profile. However, the conventional ADSA algorithms give erroneous interfacial properties when employed for a drop in externally applied electric fields. We believe this is the primary reason for absence of systematic experimental investigations in literature in electric field stimulated mass transport at liquid interfaces. We adapted ADSA for a drop under electric field by modifying Young-Laplace equation[27] and our algorithm can process a several thousand experimental drop images to return corresponding dynamic interfacial tension. To the best of our knowledge this is the first time dynamic interfacial tension of a populating interface is experimentally measured and surface excess under varied magnitudes of electric field is explicitly calculated.

Experimental Method

The experimental setup, demonstrated in Figure 1, is made up of a quartz glass cell containing electrodes, a PTFE coated stainless steel needle connected to a dosing system, and a CCD camera to capture drop profiles. The setup is similar to the one described in our previous article.[27] The electrodes are bare stainless steel plates (25 mm $\times$ 25 mm $\times$ 1 mm) placed horizontally 24 mm apart. The needle (ID = 1.1 mm and OD = 2.0 mm) is held vertical through a 3 mm hole in the upper electrode such that the equator of the drop generated at the needle tip lies equidistant from the electrodes. The lower electrode is connected to the power source consisting of a signal generator (Agilent Technologies, Model: DSO-X 2022A) and an amplifier (Trek, Model:609E-6), while the upper electrode is connected to ground. We used uniform steady DC electric fields ranging between 0 to 0.833 kV/cm.

The asphaltene sub-fractions used in this study are obtained by fractionation of whole asphaltenes extracted from a heavy crude oil from Norwegian continental shelf. The fractionation process involved passing the asphaltene solution in toluene through a calcium carbonate packed bed column.[28] The most polar sub-fraction with strongest affinity to $CaCO_3$ surface is called Irreversibly Adsorbed (IA) asphaltenes (MW = 442); whereas, the least polar asphaltenes which remain unadsorbed are called Bulk asphaltenes (MW = 508).[29] The crude oil contained about 2.8 wt% asphaltenes, of which approx. 38 wt% were Bulk asphaltenes while approx. 11 wt% were IA asphaltenes. The remaining asphaltene molecules which were weakly adsorbed are called Adsorbed asphaltenes (MW = 399).

The asphaltene sub-fractions are dissolved in xylene (98.5 %, VWR) at different concentrations which makes the medium phase. The quartz glass cell (shown in Figure 1) is filled with 20 ml organic phase. A pendent Milli-Q water drop is generated at the tip of the needle using the dosing system, which also precisely controls volume of the drop. To avoid any error in interfacial tension (IFT) measurement due to very small Bond number we used a fairly large (30 μl) drop.

The electric field is applied immediately after the drop is generated. The DC uniform

electric field is parallel to gravity and drop's vertical axis. In majority of the experiments the drop is exposed to the field for an hour. A CCD camera captured images of the drop at one frame per second speed. Every experiment is repeated for at least three times and the error bars in the figures denote standard deviations.

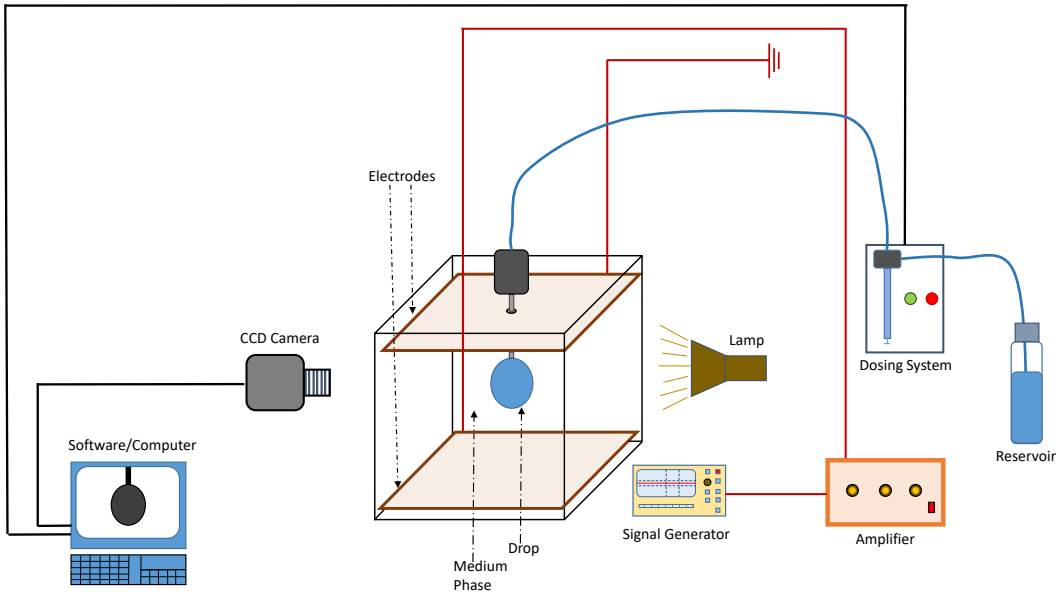

Figure 1: Schematics of the experimental setup.

IFT calculation

The experimental drop images are processed by using our in-house code for axisymmetric drop shape analysis of a drop under electric field. In axisymmetric drop shape analysis, Young-Laplace equation is used to estimate surface/interfacial tension from experimental drop profiles. A theoretical drop profiles obtained from the equation is iteratively fitted to the profile acquired from a drop image. The interfacial surface tension is calculated at the optimum fit between the two profiles. The Young-Laplace equation is given as,

$$\gamma\left(\frac{1}{R_1}+\frac{1}{R_2}\right) = \Delta p_0 - \Delta\rho g z, \tag{1}$$

where R_1, R_2 are radii of curvature, $\Delta\rho$ is density difference between drop and surrounding phases, Δp_0 is pressure difference at drop's apex and z is vertical distance from origin. When a theoretical profile is generated using Equation (1) and fitted to the experimental profile of a drop under electric field, the resulting interfacial tension can be significantly lower than the actual IFT of the interface.[27] The IFT of a clean water-xylene interface resulted from such a fitting is shown in Figure 2. The data wrongly suggests that the IFT of a clean interface linearly decreases upon increasing strength of the applied electric field. The discrepancy is a result of the drop deformation when exposed to an electric field. It can be removed by taking into account the Maxwell stresses at interface in Young-Laplace equation. We revised Young-Laplace equation in order to include the normal component of Maxwell stresses at the drop interface. In a fluid system involving a water drop surrounded by an organic solvent the tangential component of Maxwell stresses vanishes. The revised Young-Laplace equation for an aqueous drop surrounded by a dielectric liquid can be written as,

$$\gamma\left(\frac{1}{R_1}+\frac{1}{R_2}\right) = \Delta p_0 - \Delta\rho g z + \frac{1}{2}\epsilon.E_n^2. \tag{2}$$

The last term of Equation 2 is a normal component of the Maxwell stresses. ϵ and E_n represent permittivity of the medium phase and normal component of electric field at the drop interface, respectively. The electric field at the drop-oil interface is estimated using finite difference method calculations where the drop is assumed to be un-deformed at a given time step. The experimental drop profiles are used for the instantaneous drop shapes and Laplace equation for electric potential is solved outside the drop at the experimental boundary conditions.

The IFT of water-xylene interface under DC electric field, estimated with the augmented Young-Laplace equation (Equation 2), is plotted in Figure 2 along with the IFT by the conventional Young-Laplace equation (Equation 1). The IFT by the both equations are independent of time; however, when calculated by Equation 1 it is proportional to E_0. In the

absence of surface active compounds the IFT of water-xylene interface is expected to remain constant irrespective of the applied electric field strength, which is correctly estimated by Equation 2. When a surface active compound present, the IFT evolves with time. Therefore, the measurements must be done after a set time step, which is one second in our experiments.

The ADSA algorithm can process thousands of images, simultaneously returning IFT at each time step at which the images are captured. A brief discussion of the algorithm is given Appendix. The readers may refer to Mhatre *et al.*[27] for detail description of the procedure.

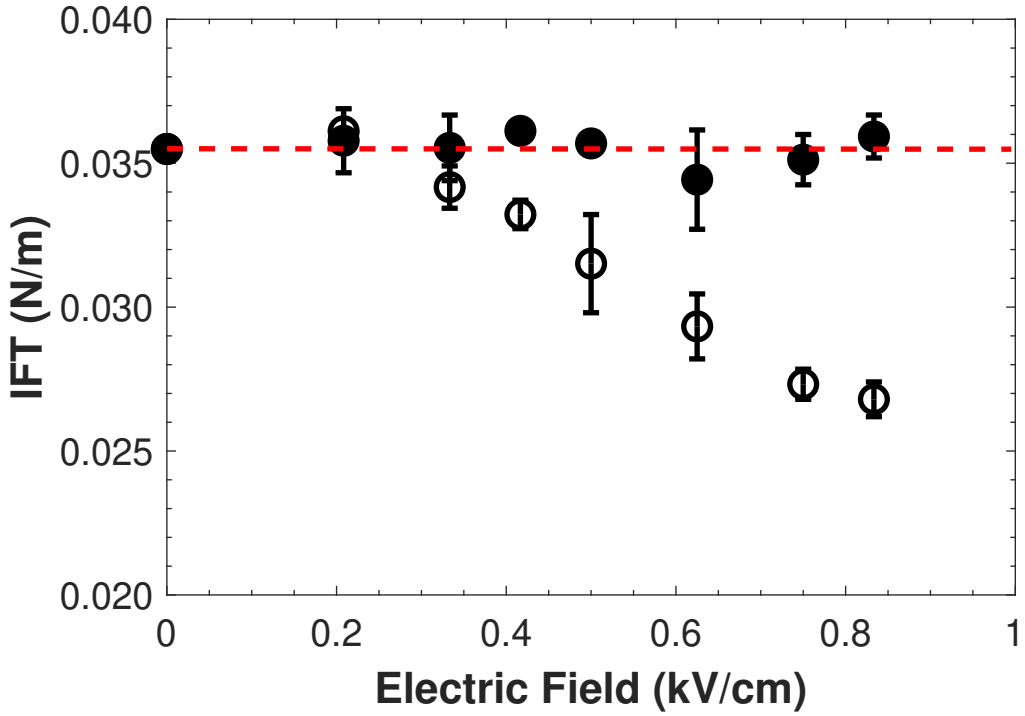

Figure 2: Interfacial tension of a clean water-xylene interface under electric field calculated with (closed symbols) and without (open symbols) including Maxwell stresses into Young-Laplace equation (after Mhatre *et al.*[27]). The dashed line represents real IFT of water-xylene interface in the absence of surface active compounds.

Results and Discussion

Interfacial Tension

The surface active molecules, present in the organic phase surrounding the drop, diffuse and adsorb to the water-oil interface resulting in the reduction in interfacial tension. Being

the most polar component of crude oil, asphaltenes easily adsorb and stabilize a water-oil interface in a crude oil emulsion. An externally applied electric field has no influence on the interfacial or rheological properties of a water-oil interface unless any surface active compound exists in the either phases. As discussed in the preceding section the dynamic interfacial tension $\gamma(t)$ of a clean water-xylene interface remains constant in an external electric field irrespective of the field strength.

A number of studies in the literature have investigated the adsorption kinetics of surface active molecules and resulting interfacial properties of the water-oil interface.[3,30,31] The surface active compounds used in our experiments- IA and Bulk asphaltenes- exhibit the similar effects on water-oil interface. Figure 3(a) shows dynamic interfacial tension of water-oil interface at different IA asphaltene concentrations (C_{IA}) in the absence of electric field. The IFT follows a steep fall immediately after the drop formation and subsequent reduction is gradual. However, eventually the interface approaches an equilibrium as IFT shows little or no change. The interfacial tension levels out as a result of an equilibrium between adsorption and desorption of the asphaltene molecules. A low C_{IA} brings about small fall in IFT while the largest concentration of IA asphaltenes $C_{IA} = 0.15$ mM reduces the IFT by more than 20 % in an hour. Contrarily, when the Bulk asphaltenes are present in medium phase the influence on IFT is observed to be marginal. The IFT attained by a water-oil interface after equilibrated for one hour at different concentrations of the asphaltenes is shown in Figure 3(b). The plots demonstrate that the decay in IFT is a strong function of asphaltene concentration in the medium phase. The observations vary for Irreversibly Adsorbed and Bulk asphaltenes. Note that the Bulk asphaltenes are the molecules that remain unadsorbed in the fractionation process due to their low affinity to $CaCO_3$. Akin to $CaCO_3$, water-oil interface does not show noticeable adsorption of this sub-fraction of asphaltenes.

In the experiments involving electric fields, the field is applied immediately after a drop is generated at the needle tip. The field is left on for an hour while camera recorded drop images after every second. The dynamic IFT calculated in Bulk and IA asphaltene solutions under

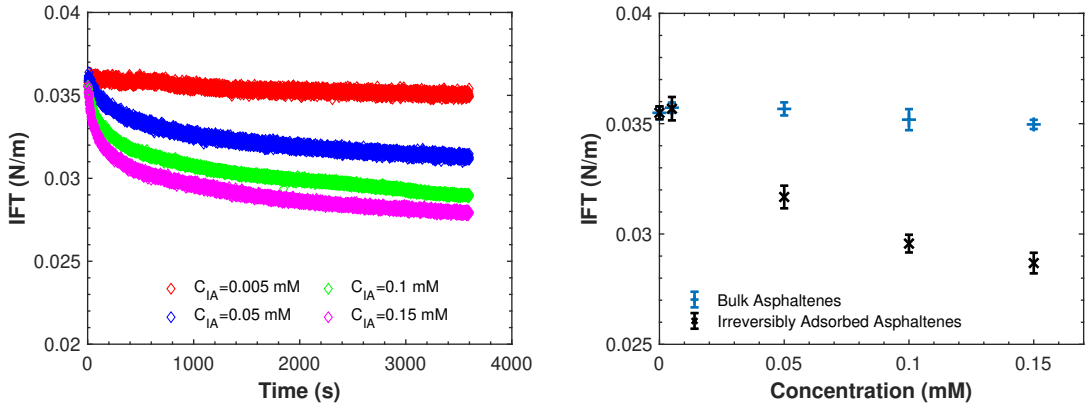

(a) (b)

Figure 3: (a) Dynamic interfacial tension of water-oil interface laden with Irreversibly Adsorbed asphaltenes at different concentrations in the absence of electric field. (b) The equilibrium interfacial tension of water-oil interface measured after one hour of aging in Bulk and IA asphaltenes at $E_0 = 0.0$ kV/cm.

electric field is plotted in Figures 4(a) and 4(b), respectively. The application of electric field does not significantly change the mass transport of Bulk asphaltenes when its concentration is low or the applied field is weak. The dynamic interfacial tension measurements presented in Figure 4(a) suggest that at concentration C_{BA}=0.005 mM the mobility and adsorption of bulk asphaltenes remain unaffected when $E_0 \leq 0.417$ kV/cm. Further increase in the applied field strength results into a sizable reduction in IFT. Upon increasing the concentration the effect becomes more prominent. Apparently, the externally applied electric field triggers the diffusion and adsorption of Bulk asphaltene molecules at water-oil interface which otherwise has a low affinity.

Contrary to Bulk asphaltenes, Irreversibly Adsorbed asphaltenes show a large and systematic decay in IFT over time. The clean interface of a freshly generated drop attracts a flurry of the molecules and the sudden crowd plummets IFT in a short time. The reduction thereafter is minor in comparison with the initial fall in IFT. The mode is similar irrespective of strength of the applied electric field, however E_0 governs the initial fall. As the dynamic IFT plots in Figure 4(b) demonstrate, the extent of reduction in IFT magnifies when E_0 is increased. Evidently the presence of electric field further intensifies the reasonably strong adsorption dynamics of IA asphaltenes at water-oil interface.

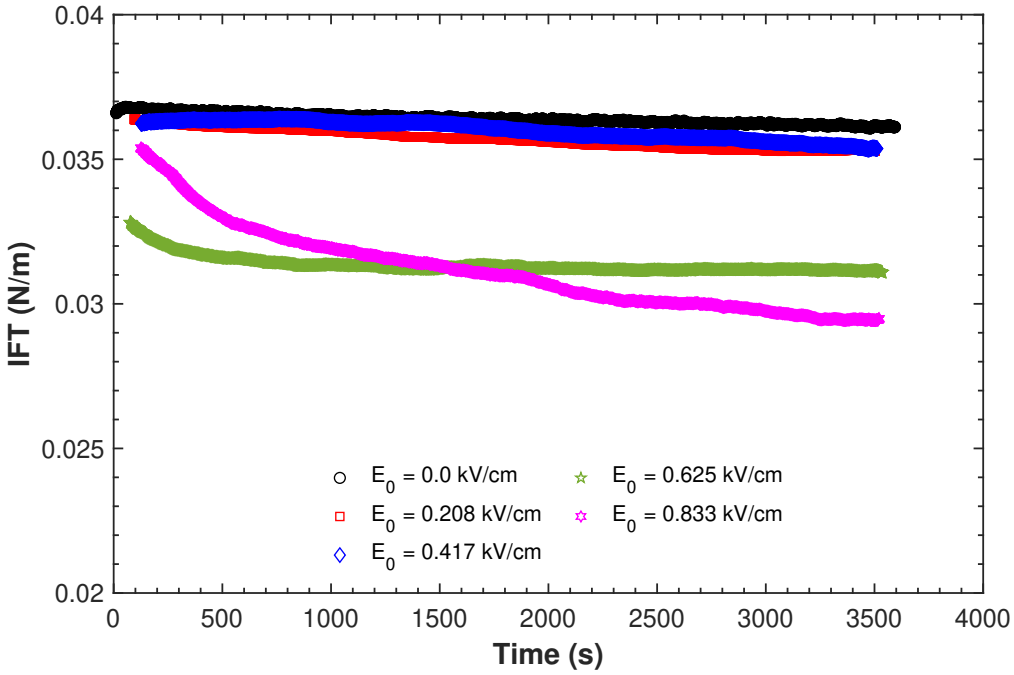

(a)

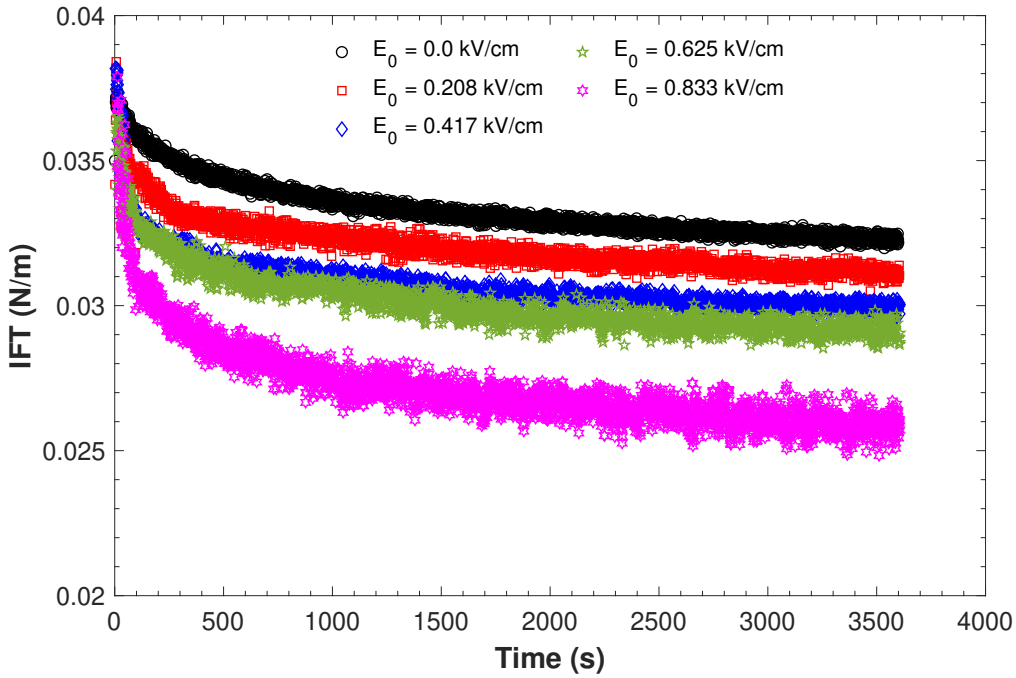

(b)

Figure 4: (a) Dynamic interfacial tension in a Bulk asphaltene solution (C_{BA} = 0.05 mM) under electric field. Curves after smoothing the original data presented in Figure 14. (b) Dynamic IFT under electric field in a bulk phase containing 0.05 mM Irreversibly Adsorbed asphaltenes.

The change in interfacial tension begins to plateau at longer times. Although it does not become constant it is safe to call the IFT after one hour an equilibrium IFT, γ_{eq}. The equilibrium IFT in an asphaltene solution decreases upon increasing strength of the applied field. As Figure 5(a) suggests γ_{eq} has a weaker influence of the field when C_{IA} is high. In C_{IA}=0.005 mM solution it drops 25 % of γ_{eq} at no field when exposed to electric field E_0=0.833 kV/cm. However, the reduction is approximately 14 % in C_{IA}=0.15 mM solution under the same field strength. Similar effects of the applied field can be observed in Bulk asphaltene solutions. Figure 5(b) shows around 20 % reduction in γ_{eq} in C_{BA}=0.05 mM solution at E_0=0.833 kV/cm from the no-field γ_{eq}, while it's around 10 % in C_{BA}=0.1 mM solution. The γ_{eq} at the all concentrations of Irreversibly Adsorbed asphaltenes converge when the electric field is stronger. No such convergence is observed in the Bulk asphaltene solutions for the range of electric field used in this study. The convergence of γ_{eq} is coherent with the previous theoretical studies which concluded that upon increasing Peclet number Sherwood number increases to a fix value. Further increase in Peclet number can be unproductive. Apparently the maximum steady Sherwood number is surfactant-specific, it is different for IA and Bulk asphaltenes.

The aforementioned reduction in equilibrium interfacial tension in the asphaltene solutions can be attributed to the electrohydrodynamic circulatory streamlines generated due to the applied electric field. As depicted in Figure 6, the streamlines appear on either sides of the water-oil interface directed from the drop's equator to poles. In the case of a pendent drop, the streamlines are axisymmetric about drop's vertical axis while the up-down symmetry is broken due the high curvature neck. The flows increase probability of asphaltene molecules coming into contact with the water-oil interface. It also increase the interfacial convections leading to denser molecular packing in the high curvature polar parts while making available more empty sites for adsorption near equator of the drop. The asphaltene adsorption at water-oil interface is irreversible.[32] As illustrated in the next section the adsorption under electric field is also irreversible and molecules occupying the interface under electric field do

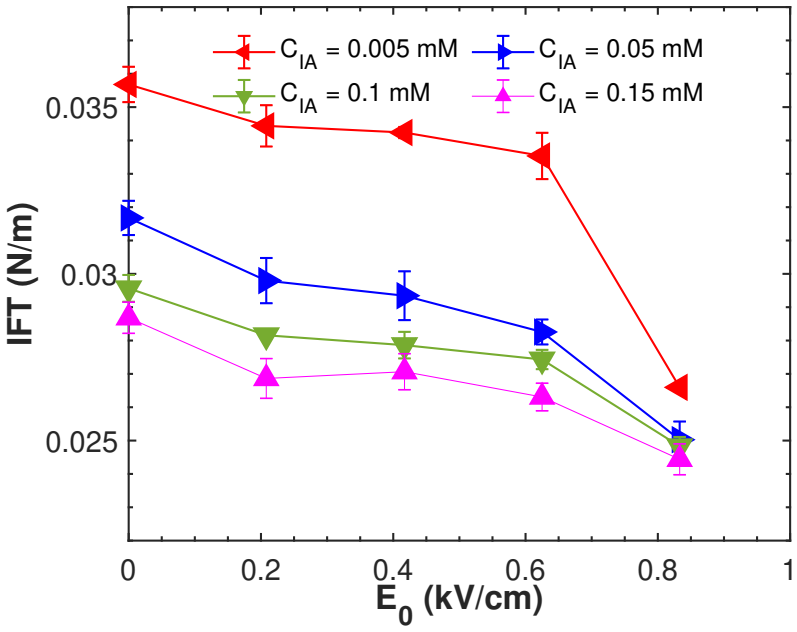

(a)

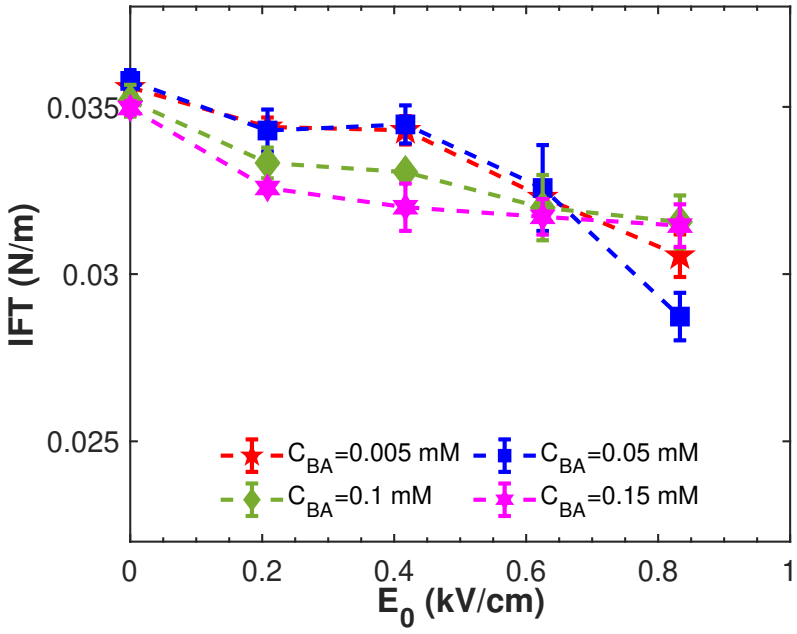

(b)

Figure 5: Equilibrium interfacial tension of water-oil interface when equilibrated under electric field for one hour at different concentrations of IA asphaltenes (a) and Bulk asphaltenes (b).

not leave after the field is switched off.

The electrohydrodynamic fluid flow velocity is directly proportional to E_0^2.[7] To demonstrate the dependence of equilibrium interfacial tension on applied electric field we scaled γ_{eq} by E_0^2. As can be seen in Figure 7, $\frac{\gamma_{eq}}{E_0^2}$ values are governed by the applied electric field and are independent of the bulk concentrations of the both asphaltene sub-fractions. The small difference in $\frac{\gamma_{eq}}{E_0^2}$ of the two sub-fractions at E_0=0.833 kV/cm diminishes at lower electric field strengths. The plots clearly indicate that the electric field-induced flows are primarily responsible for the heightened mass transport at water-oil interface, which prompts the reduction in dynamic and equilibrium interfacial tension.

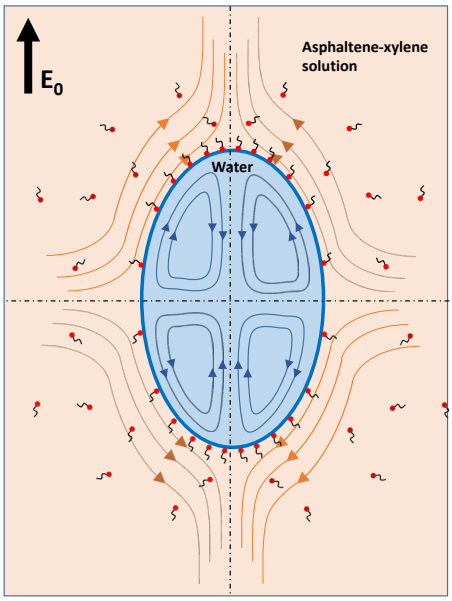

Figure 6: Schematics of electrohydrodynamic flow patterns generated at a freely suspended water drop surrounded by oil phase. The symmetric flows from the drop's equator to poles amplify the mass trasport at water-oil interface.

Diffusion Coefficient

A freshly generated drop has empty water-oil interface. It starts populating as the asphaltene molecules diffuse through the organic phase and occupy the interface. Ward and Tordai[4] assumed that the diffusing molecules enter a hypothetical subsurface next to the interface. If the interface is not fully occupied, the molecules entering into the subsurface adsorb without

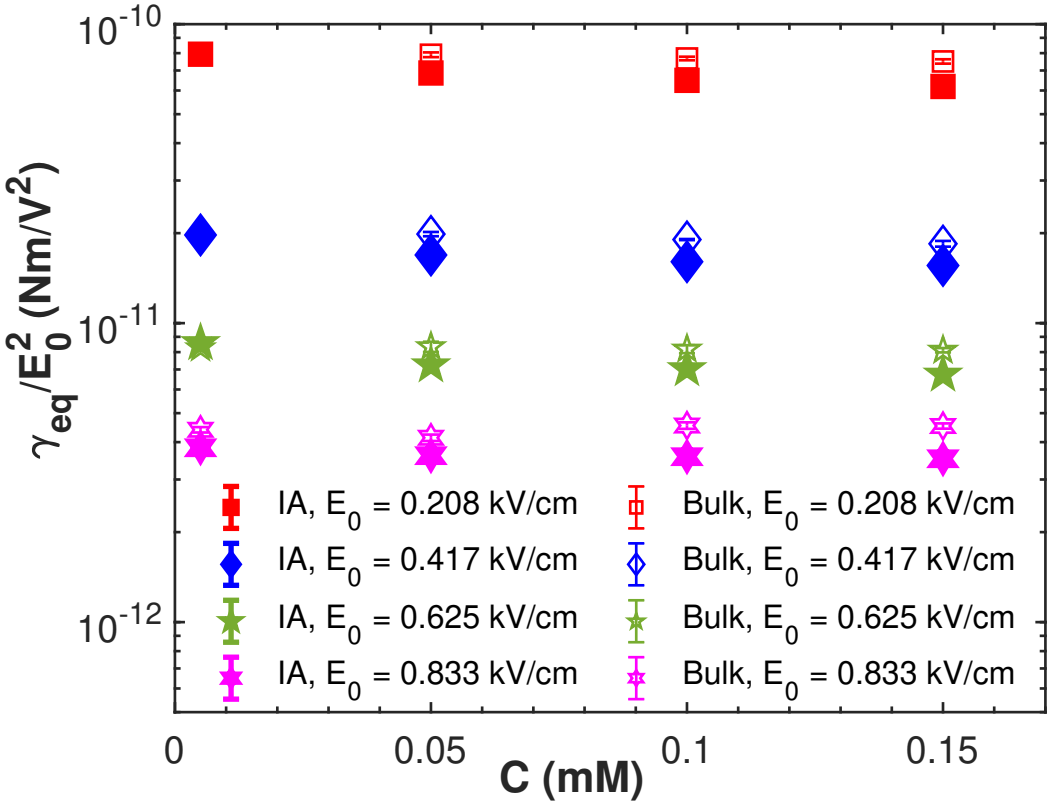

Figure 7: The equilibrium interfacial tension of water-oil interface scaled with E_0^2. The γ_{eq} is measured after 1 hour of aging in Irreversibly Adsorbed and Bulk asphlatene solutions under electric field.

resistance. However, the newly arriving molecules may diffuse back into the bulk phase when the interface is completely populated. Ward and Tordai proposed an equation for the diffusion mechanism, an asymptotic solution of which was later derived by Miller *et al.*[33] The equation can be fitted to dynamic IFT data to estimate diffusion coefficient (D) of asphaltenes at the fresh water-oil interface. The short time approximation of Ward and Tordai equation for non-ionic surface active molecules reads as,[3,33]

$$\gamma(t) = \gamma_0 - 2RTC\sqrt{Dt/\pi}. \tag{3}$$

Here γ_0, R, and T denote IFT of the clean interface, gas constant, and absolute temperature, respectively. Equation 3 is valid for the short time after formation of a fresh interface.

Equation 3 is fitted to experimental dynamic interfacial tension data to estimate diffusion coefficient of asphaltenes in the presence and absence of the electric fields. The fitting of

Equation 3 to the experimental IFT is demonstrated in Figure 8. In the absence of electric field the molecular adsorption is slow and steady despite the initial heavy crowding at the interface. Therefore the IFT data is in agreement with Equation 3 over a longer time as compared to γ in electric field. When the electric field is present at the time of drop formation, the initial adsorption is rapid and the IFT falls substantially in a short time. The subsequent adsorption is gradual and similar to the long term no-electric field adsorption. The difference in the initial mass transport can be attributed to the electric field induced streamlines which increase the probability of asphaltenes to reach the interface and populate it more in comparison with the interface without field.

The diffusion coefficient estimated in this work is at the beginning of electric field application when the interface is empty and mass transport is diffusion controlled. After the interface is substantially crowded, the molecules entering into the subsurface experience barrier due to the already adsorbed molecules. At this stage a fraction of the molecules entering the subsurface diffuse back into the bulk phase. This mass transfer is considered mixed kinetic-diffusion controlled. The diffusion coefficient values presented here are calculated by short-time approximation of Ward and Tordai equation for diffusion controlled mass transport. The good agreement (Figure 8) between the equation and experimental IFT at short times after application of electric field is an indication of the diffusion controlled adsorption even under influence of electric field. However, in the presence of an electric field the interface occupies quickly and the fitting starts deviating as the diffusion controlled mechanism turns into mixed kinetic-diffusion controlled. Whereas, this transition delays when electric field is absent. Note that Ward and Tordai equation is based on an assumption that the molecular adsorption occurs through diffusion;[4] however, given the presence of electrohydrodynamic flows the adsorption may not be purely diffusion controlled under electric fields. Therefore, the improved diffusion cofficient thus obtained is henceforth termed as effective diffusion coefficient.

The effective diffusion coefficients (D) at different concentrations and electric field strengths

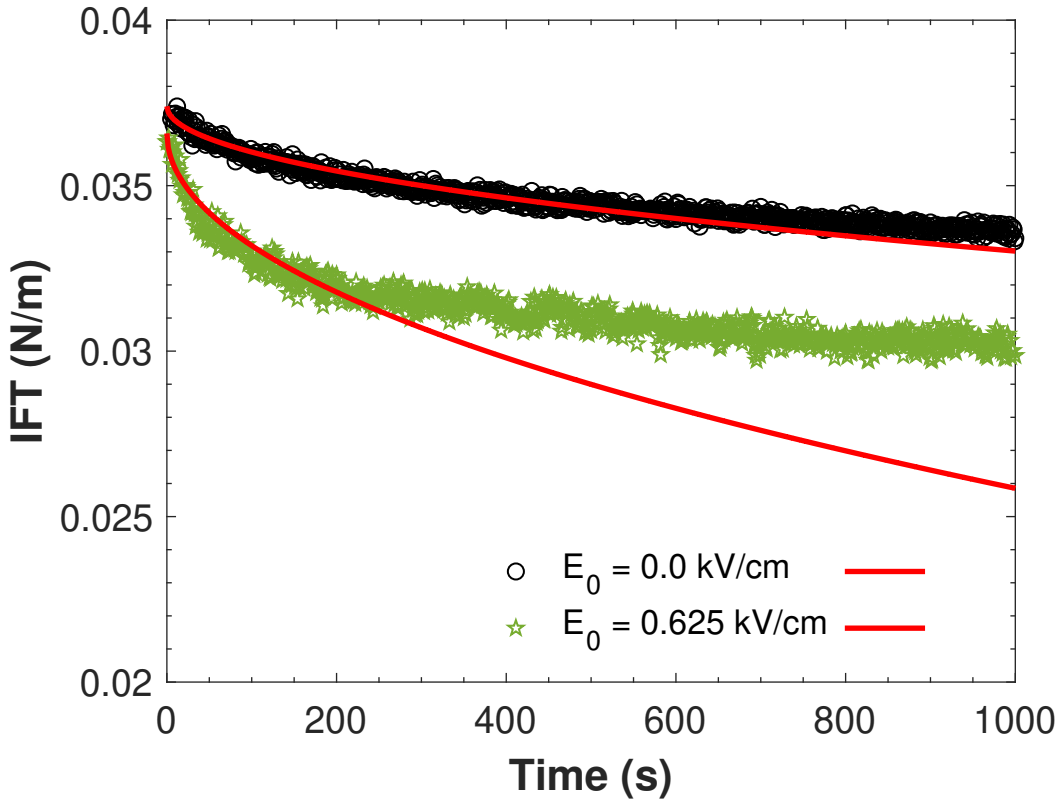

Figure 8: Diffusion coefficient estimation by fitting short time approximation of Ward and Tordai equation (——) to dynamic interfacial tension of water-oil interface in C_{IA}=0.05 mM solution in the absence of electric field and at E_0=0.625 kV/cm.

is calculated using Equation 3. The diffusion coefficients of the asphaltenes are observed to be higher in a system under electric field than that in no-field case. The estimated values of D of IA asphaltenes show a marginal increase with the field strength when the concentrations are higher (C_{IA} = 0.05, 0.1 and 0.15 mM). However, the concentrations of the both sub-fractions of asphaltenes, at which the dynamic interfacial tension otherwise shows a minuscule decay, D appears to be ramping up with E_0. Although the no-field diffusion coefficients of Bulk asphaltenes are very small as compared to D of IA asphaltenes, the effect of electric field on the former is turned out to be more intense. The estimated D of the both sub-fractions demonstrate that the low-affinity Bulk asphaltenes and IA asphaltenes at low concentrations barely self-diffuse and adsorb to the water-oil interface. This is also evident from the low γ_{eq} values in Figures 5(a) and 5(b). The application of electric field and the resulting convection help the molecules to reach empty sites at the interface which is reflected by the decay in

the interfacial tension.

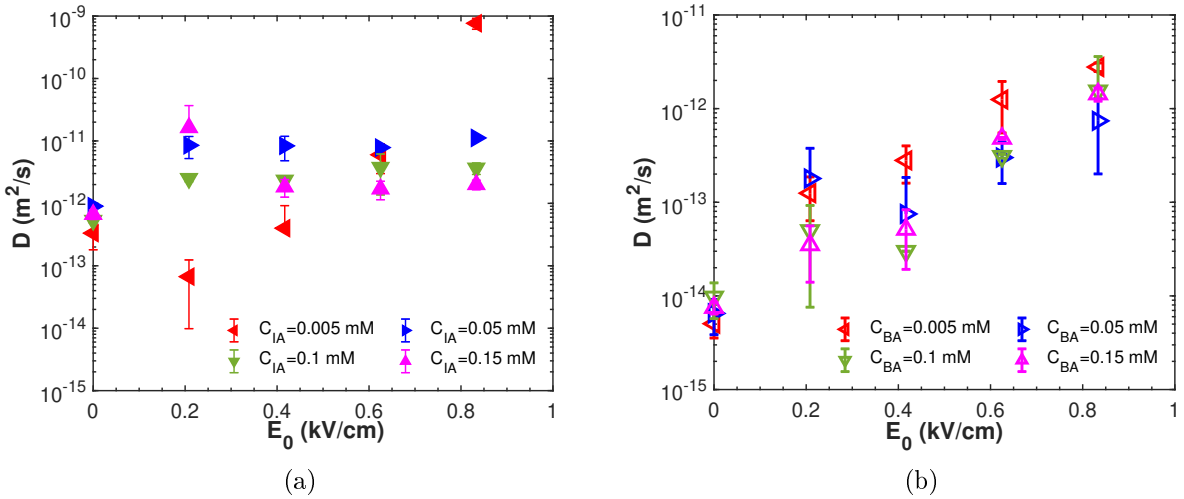

(a) (b)

Figure 9: The effective diffusion coefficient of asphaltenes at fresh water-oil interface under electric field, (a) Irreversibly Adsorbed asphaltenes and (b) Bulk asphaltenes.

Surface excess

Following in footsteps of Eastoe *et al.*,[30] we calculated the surface excess at E_0 by using the γ_{eq} data and Gibb's isotherm,

$$\Gamma = -\frac{1}{RT}\frac{d\gamma}{d\ ln(C)}. \tag{4}$$

The equilibrium interfacial tension, presented in Figures 5(a) and 5(b), fit well to a cubic function as demonstrated in Figure 10(a). The γ_{eq} vs C at each strength of the applied electric field is fitted and tangent to the resulting cubic functions at each C are used to solve Equation 4. The estimated Γ is plotted against asphaltene concentrations as demonstrated in Figure 10(b) which gives the equilibrium surface excess Γ_{eq} at the plateau. The equilibrium surface excess of Irreversibly Adsorbed asphaltenes calculated at each E_0 is plotted in Figure 10(c). Apparently the applied electric field magnifies the amount of asphaltenes accumulate at the interface. The Γ_{eq} shows relatively small increments at weaker field strengths, but at $E_0 = 0.833$ kV/cm it is 1.57 times Γ_{eq} in the absence of field.

The asphaltene adsorption in the absence of external forces is irreversible.[25,34] Similarly,

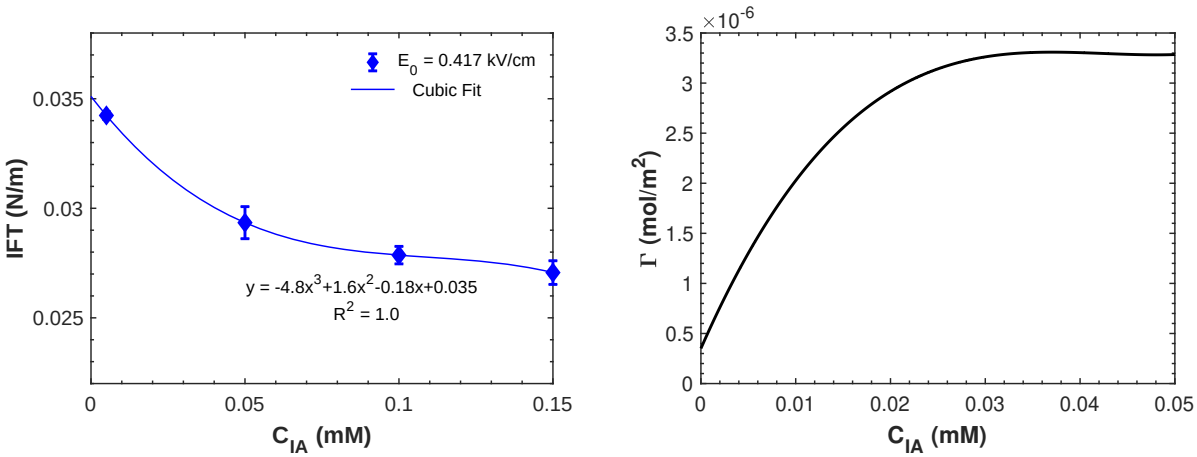

(a) (b)

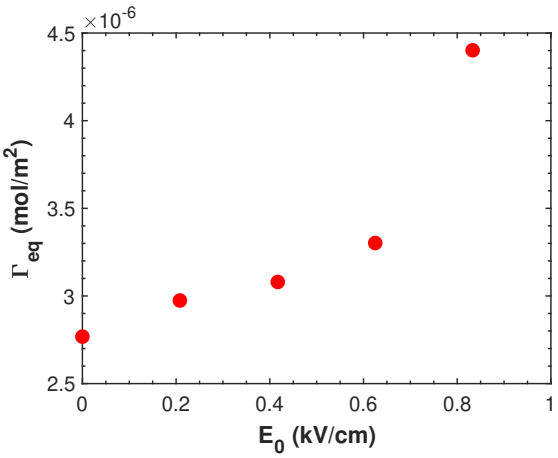

(c)

Figure 10: (a) The interfacial tension of water-oil interface measured after 1 hour aging in IA asphaltene solutions under electric field E_0=0.417 kV/cm. (b) Surface excess, estimated by using Equation 4, versus concentration of Irreversibly Adsorbed asphaltenes at E_0=0.417 kV/cm. The Γ vs C plots plateau at Γ_{eq}, the surface concentration of asphaltenes at equilibrium. (c) The equilibrium surface excess (Γ_{eq}) of IA asphaltenes at water-oil interface when exposed to uniform DC electric field E_0.

the asphaltene molecules adsorbed while electric field is on do not desorb if the field turned off. As can seen in Figure 11, for the both asphaltene sub-fractions, interfacial tension of water-oil interface decays in the beginning while electric field is on. After one hour when the field is switched off, the IFT remains approximately constant. In Bulk asphaltene solution C_{BA}= 0.1 mM, although the reduction in IFT after an hour under E_0=0.417 kV/cm is minor, it does not increase for the next hour when the field is kept off. While the water-oil IFT in C_{IA}= 0.1 mM solution falls significantly when put in electric field E_0=0.417 kV/cm for one hour, it displays similar tendency against recovery after the field is switched off. Evidently the molecular adsorption responsible for the reduction in IFT under electric field is irreversible and the molecules after occupying the empty sites at the interface do not desorb and diffuse back into the bulk phase when the field is switched off.

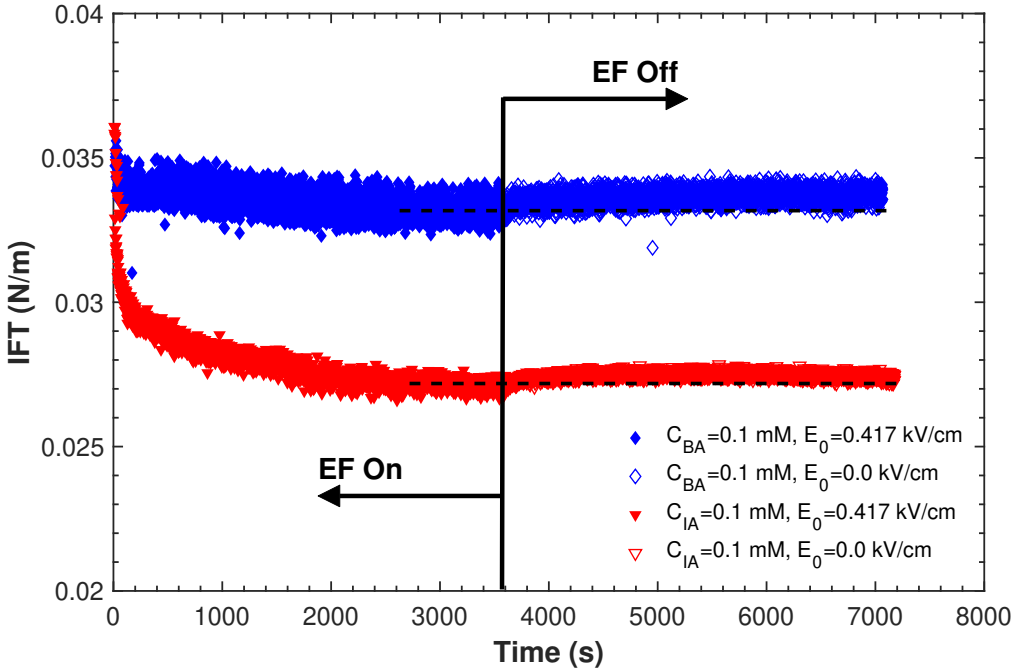

Figure 11: Irreversible adsorption of asphaltenes under electric field. IFT of a freshly generated water drop surrounded by an asphaltene solution under electric field E_0=0.417 kV/cm for an hour, followed by an hour without field.

Another important aspect of the interface that's observed to be changed after a drop left in a concentrated solution under a strong electric field is its appearance. A drop interface appeared darker after aging into 0.1 and 0.15 mM Irreversibly Adsorbed asphaltene solutions

under strong electric fields. As can be seen in Figure 12, on the image of a freshly generated drop in 0.15 mM IA asphaltene solution the bright part in the center is a result of the light reflected from the drop's surface. The bright area turned partially dark after the drop left to age in the solution under electric field E_0=0.417 kV/cm. However, in the absence of the field no such change is observed in the end of aging. We believe that this difference is an indication of greater extent of adsorption under electric field as the highly populated interface does not reflect light.

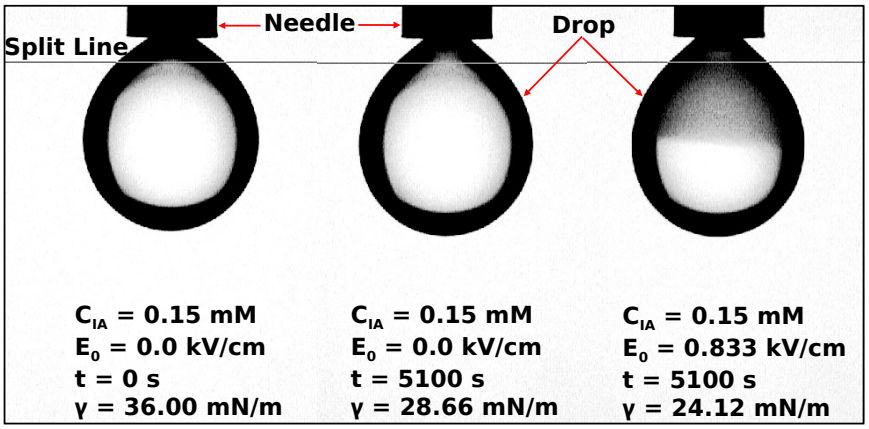

Figure 12: Drop appearances in an IA asphaltene solution aged at different conditions.

Conclusions

In this work we present systematic experiments in adsorption of asphaltenes at a pendent drop interface exposed to a DC electric field. Temporal images of the water drop, surrounded by an asphaltene-rich organic phase, are processed using ADSA algorithm to estimate dynamic interfacial tension. Two sub-fractions of asphaltenes with distinct affinities to water-oil interface show dissimilar influence on the IFT in the presence as well as absence of the electric field. However, when the system is put under electric field, adsorption dynamics of the

both sub-fractions considerably intensify. The effect is evident from the lower dynamic and equilibrium interfacial tensions at a stronger electric field. The decay in IFT converges above a reasonably strong electric field and in the case of IA asphaltenes, at E_0=0.833 kV/cm it reaches comparable values at all concentrations studied. The data is consistent with theoretical studies in the literature and suggests that the maximum steady Sherwood number can be dependent on a surfactant.

The convective mass flux due to the electrohydrodynamic flows is proportional to the concentration gradient as well as fluid flow. The two are collectively effective when the interface is fresh and less crowded; while the electric field induced flows are particularly responsible for the mass transport at the longer times. The scaling of γ_{eq} data by E_0^2 suggests that the intensified asphaltene adsorption is essentially due to the electric field-induced fluid flows and independent of the bulk concentration. The flows help asphaltene molecules make it to the interface faster and to amply pack the interface when the field is adequately strong. The molecules once adsorbed under electric field do not desorb after the field in switched off. The effective diffusion coefficient of the asphaltenes at a fresh interface, calculated by fitting Ward and Tordai equation, is found to be larger under stronger electric field. Similarly, the maximum surface excess ramps up with E_0, suggesting more amount of asphaltenes accumulated at drop interface under a stronger electric field.

The excess mass transport of surface active molecules due to the presence of electric field has pertinence in multiphase systems including emulsions, aerosols and foams. We are confident that the results presented here will shed light on the stability of fluid interfaces in the electric field –based applications such as electrocoalescence, electrocoagulation, microfluidics, electro-emulsification, electrostatic atomization, etc. For instance, during coalescence of two droplets in the presence of electric field and surface active compounds, the evolved interfacial properties govern kinetics of the coalescence.[34–36] In the electric field controlled microfluidic applications such as microreactor technology,[37] bioparticle handling,[38] assay,[39] etc., future studies could investigate enhancement in the mass transport at/across the interfaces.

Acknowledgement

The authors thank the JIP Electrocoalescence consortium "New Strategy for Separation of Complex Water-in-Crude Oil Emulsions: From Bench to Large Scale Separation (NFR PETROMAKS)", consisting of Ugelstad Laboratory (NTNU, Norway), University of Alberta (Canada), Swiss Federal Institute of Technology in Zurich (Switzerland), Institutt for energiteknikk (Norway) and funded by Norwegian Research Council (Grant255174) and the following industrial sponsors – Nouryon, Anvendt Teknologi AS, NalcoChampion, Equinor, and Sulzer.

Appendix

ADSA algorithm

The calculation of dynamic interfacial tension with axisymmetric drop shape analysis (ADSA) involves generation of a theoretical drop profile and fitting it iteratively to an experimentally acquired profile. The conventional Young-Laplace equation is augmented to consider Maxwell stresses at water-oil interface when the drop is put into externally applied electric field. The equation (Equation 2 in main body) is written as,

$$\gamma\left(\frac{1}{R_1}+\frac{1}{R_2}\right) = \Delta p_0 - \Delta\rho g z + \frac{1}{2}\epsilon.E_n^2. \tag{5}$$

Equation 5 is non-dimensionalized and expressed in terms of gravitational Bond number ($\beta = b^2\Delta\rho g/\gamma$) and electric Bond number ($\beta_e = V_0^2\epsilon/b\gamma$). Here, V_0 is electric potential applied at the lower electrode and b is drop's radius of curvature at its apex.

The electric field at the drop interface is estimated by solving two dimensional Laplace equation for electric potential outside the drop at each time step. The finite difference method is used to calculate the equation along with actual experimental boundary conditions. The

electric field thus obtained is used get the normal component of Maxwell stress at the drop interface.

The cartesian coordinates of the experimental drop profile at t = 0 s and an initial guess for gravitational Bond number (β_0) are inputs for the ADSA algorithm. The coordinates are used to estimate E_n at the interface (at t = 0 s) assuming the drop undeformable. A theoretical profile is generated using equation 2 based on β_0. The profile is iteratively fitted to the experimental profile at t = 0 s and the fit is optimized by updating β_0 until the two profiles are matched. The best fit between the experimental and theoretical drop profiles is demonstrated in Figure 13. The interfacial tension is calculated from the β_0 at the optimum fit ($\gamma = b^2 \Delta\rho g/\beta_0$). The IFT at the next time step is calculated similarly, with β estimated in the previous step as β_0.

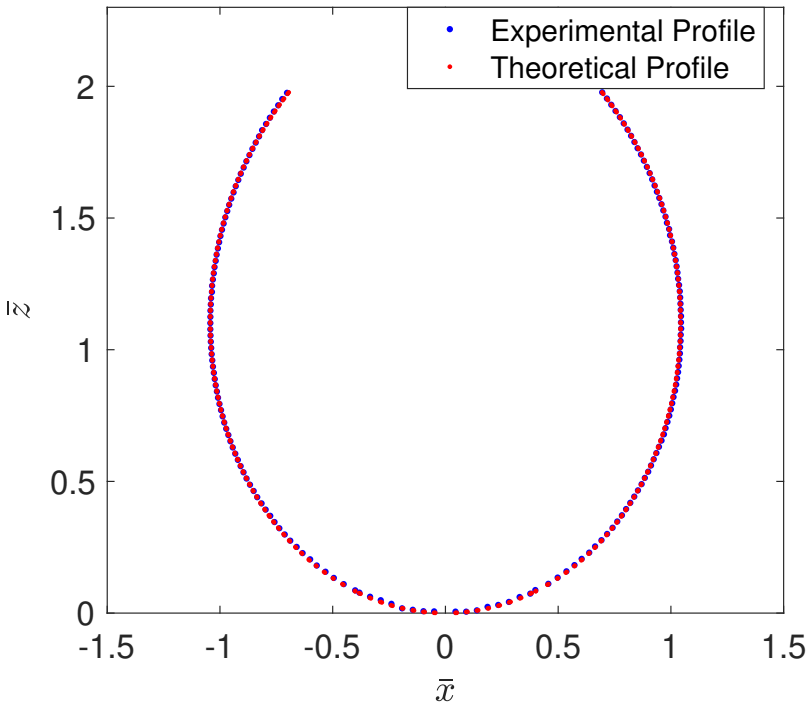

Figure 13: Optimum fit between experimental and theoretical profiles of a 30 μl pendent water drop surrounded by xylene under 0.625 kV/cm electric field. $\bar{x}$ and $\bar{z}$ are radial and vertical coordinates, respectively, scaled by radius of curvature of the drop at its apex.

Raw IFT data

The dynamics interfacial tension data in bulk asphaltene solution under electric field obtained by the ADSA algorithm is scattered. To illustrate the real trends we presented time-averaged plots in main part of the manuscript. The IFT raw data is shown in Figure 14.

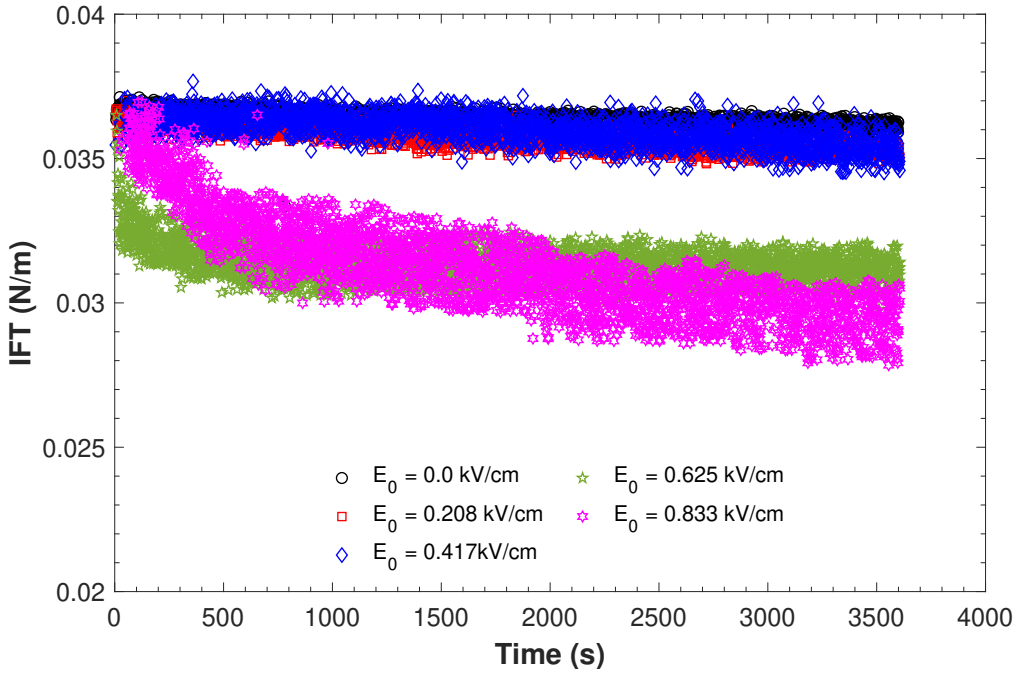

Figure 14: Dynamic interfacial tension in a Bulk asphaltene solution (C_{BA} = 0.05 mM) under electric field (Original data).

Table 1: γ_{eq}/E_0^2 data (presented in Figure 7) in Irreversibly Adsorbed and Bulk asphaltene solutions under electric field. Average values are followed by standard deviations in brackets.

E_0 / **C (mM)**	**0.208 kV/cm**	**0.417 kV/cm**	**0.625 kV/cm**	**0.833 kV/cm**
C_{IA}=**0.005**	0.7935×10^{-10} (0.1426×10^{-11})	0.6866×10^{-10} (0.1563×10^{-11})	0.6488×10^{-10} (0.0046×10^{-11})	0.6189×10^{-10} (0.1374×10^{-11})
C_{IA}=**0.05**	0.1972×10^{-10} (0.0965×10^{-12})	0.169×10^{-10} (0.4215×10^{-12})	0.1605×10^{-10} (0.2297×10^{-12})	0.1559×10^{-10} (0.3113×10^{-12})
C_{IA}=**0.1**	0.8585×10^{-11} (0.1778×10^{-12})	0.7234×10^{-11} ($0.0.0958\times10^{-12}$)	0.7022×10^{-11} (0.0742×10^{-12})	0.6735×10^{-11} (0.1057×10^{-12})
C_{IA}=**0.15**	0.3830×10^{-11} (0.1225×10^{-13})	0.3604×10^{-11} (0.7855×10^{-13})	0.3575×10^{-11} (0.4029×10^{-13})	0.3519×10^{-11} (0.6675×10^{-13})
C_{BA}=**0.005**	0.7926×10^{-10} (0.0652×10^{-11})	0.7902×10^{-10} (0.1446×10^{-11})	0.7678×10^{-10} (0.1059×10^{-11})	0.7506×10^{-10} (0.1267×10^{-11})
C_{BA}=**0.05**	0.1976×10^{-10} (0.2444×10^{-12})	0.1986×10^{-10} (0.3278×10^{-12})	0.1904×10^{-10} (0.0812×10^{-12})	0.1843×10^{-10} (0.4073×10^{-12})
C_{BA}=**0.1**	0.8269×10^{-11} (0.1086×10^{-12})	0.8339×10^{-11} (0.3288×10^{-12})	0.8189×10^{-11} (0.2500×10^{-12})	0.8119×10^{-11} (0.1365×10^{-12})
C_{BA}=**0.15**	0.4399×10^{-11} (0.0916×10^{-12})	0.4137×10^{-11} (0.1023×10^{-12})	0.4545×10^{-11} (0.1140×10^{-12})	0.4529×10^{-11} (0.0916×10^{-12})

References

(1) He, Y.; Yazhgur, P.; Salonen, A.; Langevin, D. Adsorption–desorption kinetics of surfactants at liquid surfaces. *Adv. Colloid Interface Sci.* **2015**, *222*, 377 – 384.

(2) Lin, S.-Y.; Lu, T.-L.; Hwang, W.-B. Adsorption Kinetics of Decanol at the Air-Water Interface. *Langmuir* **1995**, *11*, 555–562.

(3) Eastoe, J.; Dalton, J. S. Dynamic surface tension and adsorption mechanisms of surfactants at the air–water interface. *Adv. Colloid Interface Sci.* **2000**, *85*, 103 – 144.

(4) Ward, A. F. H.; Tordai, L. Time-Dependence of Boundary Tensions of Solutions I. The Role of Diffusion in Time-Effects. *J. Chem. Phys* **1946**, *14*, 453–461.

(5) Taylor, G. Studies in Electrohydrodynamics. I. The Circulation Produced in a Drop by Electrical Field. *Proc. R. Soc. London, Ser. A* **1966**, *291*, 159–166.

(6) Morrison, J., F. A. Transient Heat and Mass Transfer to a Drop in an Electric Field. *J. Heat Transfer* **1977**, *99*, 269–273.

(7) Griffiths, S. K.; Morrison, F. A. J. Low Peclet Number Heat and Mass Transfer from a Drop in an Electric Field. *ASME. J. Heat Transfer.* **1979**, *101*, 484–488.

(8) Oliver, D. L.; Carleson, T. E.; Chung, J. N. Transient heat transfer to a fluid sphere suspended in an electric field. *Int. J. Heat Mass Transfer* **1985**, *28*, 1005 – 1009.

(9) Oliver, D.; De Witt, K. High Peclet number heat transfer from a droplet suspended in an electric field: interior problem. *Int. J. Heat Mass Transfer* **1993**, *36*, 3153–3155.

(10) Abdelaal, M. R.; Jog, M. A. Steady and time-periodic electric field-driven enhancement of heat or mass transfer to a drop: Internal problem. *Int. J. Heat Mass Transfer* **2012**, *55*, 251–259.

(11) Abdelaal, M.; Jog, M. Heat/mass transfer from a drop translating in steady and time-periodic electric fields: External problem. *Int. J. Heat Mass Transfer* **2012**, *55*, 2315–2327.

(12) Abdelaal, M. R.; Jog, M. A. Heat/mass transport in a drop translating in time-periodic electric fields. *Int. J. Heat Mass Transfer* **2013**, *66*, 284 – 294.

(13) Moriya, S.; Adachi, K.; Kotaka, T. Deformation of droplets suspended in viscous media in an electric field. 1. Rate of deformation. *Langmuir* **1986**, *2*, 155–160.

(14) Adachi, K.; Tanaka, M.; Shikata, T.; Kotaka, T. Deformation of viscoelastic droplet in an electric field. 1. Aqueous cetyltrimethylammonium bromide-sodium salicylate solution in poly(dimethylsiloxane). *Langmuir* **1991**, *7*, 1281–1286.

(15) Carleson, T. E. *Drop oscillation and mass transfer in alternating electric fields*; 1992; Vol. 93; p 17086.

(16) He, W.; Baird, M. H. .; Chang, J. S. The effect of electric field on mass transfer from drops dispersed in a viscous liquid. *Can. J. Chem. Eng.* **1993**, *71*, 366–376.

(17) Schmid, G. M.; Hurd, R. M.; S., S. J. E. Effects of Electrostatic Fields on the Surface Tension of Salt Solutions. *J. Electrochem. Soc.* **1962**, *109*, 852–858.

(18) Blank, M.; Feig, S. Electric Fields across Water-Nitrobenzene Interfaces. *Science* **1963**, *141*, 1173–1174.

(19) Hayes, C. F. Water-air interface in the presence of an applied electric field. *The Journal of Physical Chemistry* **1975**, *79*, 1689–1693.

(20) Moriya, S.; Kawamoto, S.; Urakawa, O.; Adachi, K. Study of interfacial tension in poly(ethylene oxide)/polystyrene/diblock copolymer system by electric deformation method. *Polymer* **2006**, *47*, 6236 – 6242.

(21) Degen, P.; Chen, Z.; Rehage, H. Stimulated Deformation of PolysiloxaneCapsules in External Electric Fields. *Macromol. Chem. Phys.* **2010**, *211*, 434–442.

(22) Weatherley, L.; Petera, J.; Qiu, Z. Intensification of mass transfer and reaction in electrically disturbed liquid-liquid systems. *Chem. Eng. J.* **2017**, *322*, 115 – 128.

(23) Mhatre, S.; Simon, S.; Sjöblom, J. Shape evolution of a water drop in asphaltene solution under weak DC electric fields. *Chem. Eng. Res. Des.* **2019**, *141*, 540–549.

(24) Sjoblom, J.; Aske, N.; Auflem, I. H.; Brandal, O.; Havre, T. E.; Saether, O.; Westvik, A.; Johnsen, E. E.; Kallevik, H. Our current understanding of water-in-crude oil emulsions Recent characterization techniques and high pressure performance. *Adv. Colloid Interface Sci.* **2003**, *100*, 399 – 473.

(25) Freer, E. M.; Radke, C. J. Relaxation of asphaltenes at the toluene/water interface: Diffusion exchange and surface rearrangement. *J. Adhesion* **2004**, *80*, 481–496.

(26) Mhatre, S.; Vivacqua, V.; Ghadiri, M.; Abdullah, A.; Al-Marri, M.; Hassanpour, A.; Hewakandamby, B.; Azzopardi, B.; B., K. Electrostatic phase separation: A review. *Chem Eng Res Des* **2015**, *96*, 177–195.

(27) Mhatre, S.; Simon, S.; Sjöblom, J. Methodology to calculate interfacial tension under electric field using pendent drop profile analysis. *Proc. R. Soc. London, Ser. A* **2019**, *475*, 20180852.

(28) Ruwoldt, J.; Subramanian, S.; Simon, S.; Oschmann, H.; Sjöblom, J. Asphaltene fractionation based on adsorption onto calcium carbonate: Part 3. Effect of asphaltenes on wax crystallization. *Colloids Surf., A* **2018**, *554*, 129 – 141.

(29) Pinto, F. E.; Barros, E. V.; Tose, L. V.; Souza, L. M.; Terra, L. A.; Poppi, R. J.; Vaz, B. G.; Vasconcelos, G.; Subramanian, S.; Simon, S.; Sjöblom, J.; Romão, W. Fractionation of asphaltenes in n-hexane and on adsorption onto CaCO3 and characterization by ESI(+)FT-ICR MS: Part I. *Fuel* **2017**, *210*, 790 – 802.

(30) Eastoe, J.; Dalton, J. S.; Rogueda, P. G. A.; Crooks, E. R.; Pitt, A. R.; Simister, E. A. Dynamic Surface Tensions of Nonionic Surfactant Solutions. *J. Colloid Interface Sci.* **1997**, *188*, 423 – 430.

(31) Sztukowski, D. M.; Yarranton, H. W. Rheology of AsphalteneToluene/Water Interfaces. *Langmuir* **2005**, *21*, 11651–11658.

(32) Kilpatrick, P. K.; Spiecker, P. M. In *Encyclopedic Handbook of Emulsion Technology*; Sjöblom, J., Ed.; Marcel Dekker: New York, 2001; pp 707–730.

(33) Fainerman, V.; Makievski, A.; Miller, R. The analysis of dynamic surface tension of sodium alkyl sulphate solutions, based on asymptotic equations of adsorption kinetic theory. *Colloids Surf., A* **1994**, *87*, 61 – 75.

(34) Mhatre, S.; Hjartnes, T.; Simon, S.; Sjöblom, J. Coalescence Behavior of Stable Pendent Drop Pairs Held at Different Electric Potentials. *Langmuir* **2020**, *36*, 1642–1650.

(35) Niu, X.; Gielen, F.; deMello, A. J.; Edel, J. B. Electro-Coalescence of Digitally Controlled Droplets. *Anal. Chem.* **2009**, *81*, 7321–7325.

(36) Hjartnes, T. N.; Mhatre, S.; Gao, B.; Sørland, G. H.; Simon, S.; Sjöblom, J. Demulsification of crude oil emulsions tracked by pulsed field gradient NMR. Part II: Influence of chemical demulsifiers in external AC electric field. *Colloids Surf., A* **2020**, *586*, 124188.

(37) Link, D. R.; Grasland-Mongrain, E.; Duri, A.; Sarrazin, F.; Cheng, Z.; Cristobal, G.; Marquez, M.; Weitz, D. A. Electric Control of Droplets in Microfluidic Devices. *Angew. Chem. Int. Ed.* **2006**, *45*, 2556–2560.

(38) Ng, A. H.; Li, M. D. W. A. R., B. B.and Chamberlain Digital Microfluidic Cell Culture. *Annu Rev Biomed Eng.* **2015**, *17*, 91-112.

(39) Chokkalingam, V.; Ma, Y.; Thiele, J.; Schalk, W.; Tel, J.; Huck, W. T. An electro-coalescence chip for effective emulsion breaking in droplet microfluidics. *Lab Chip.* **2014**, *14*, 2398-2402.

For Table of Contents Only